Proc. XXX IAHR Congress (accepted)

A non-hydrostatic numerical modelling of exchange flows

Yuliya Kanarska[1], Vladimir Maderich [1,2]

[1)] Institute of Mathematical Machine and System Problems, Glushkova av. 42, 03187 Kiev, Ukraine. [2)] Ukrainian Center of Environmental and Water Projects, Kiev, Ukraine
tel. (38044)2666187 fax. (38044)2663615 e-mail: kanarska@ukrpost.net

Abstract

Stratified exchange flows are investigated by a three-dimensional, non-hydrostatic, numerical model with a free surface. The model is based on 3D Reynolds-averaged Navier-Stokes equations under the Boussinesq assumption. The model equations are written in a generalized vertical coordinate system and with orthogonal curvilinear horizontal coordinates. A mode splitting technique, decomposition of pressure and velocity fields into hydrostatic and non-hydrostatic components and sequential calculation of these components are the base of numerical algorithm of the model. The model was tested against a laboratory experiment on the exchange flow through long and narrow strait and was applied to simulate the water exchange through the Strait of Dardanelles. It reproduces the complicated three-dimensional structures of currents in the Dardanelles. It also shows that mixing plays a crucial role in maintaning the observed exchange flow between the Aegean and Marmara seas.

Keywords Computational hydraulics, exchange flow, mixing, Strait of Dardanelles

1. Introduction

Non-hydrostatic effects are essential in a wide spectrum of coastal hydraulic problems. Examples may be found in flows with steep waves progressing over nonuniform bottom in coastal areas, in buoyant plumes from submerged outfalls, in breaking internal waves of large amplitude generated by tidally driven flows over a steep topography, etc. An important class of stratified flows is the exchange flow between water bodies driven by density and level differences. Such bidirectional flows take place in sea straits. According to hydraulic theory (Armi and Farmer, 1986; Farmer and Armi, 1986) the exchange flows are limited by topographic constrictions (sills and contractions) that hydraulically control exchange. Recent studies showed the importance of non-hydrostatic forces in the dynamics of exchange flows (Zhu and Lawrence, 1998). Friction and mixing are also essential in long and shallow straits (Hogg et al., 2001). Therefore, classical hydraulical analysis should be extended to include non-hydrostatic effects and the entrainment. The 3D non-hydrostatic modelling allows investigation of the complicated and interrelated effects of strait topography, level changes and of the profiles of temperature and salinity in the adjacent seas on the exchange flows, mixing and hydraulic control. In this paper the 3D non-hydrostatic numerical model of Kanarska and Maderich (2002a; 2002b) is applied for modeling the lock-exchange flows and exchange flows through sea straits. The model is a non-hydrostatic extension of free-surface primitive equation POM model (Blumberg and Mellor, 1987). It has been tested against the laboratory experiments of Maderich (2000) and the DNS simulations of Hartel et al. (2000). The model is applied for investigating the 3D flow structure, the density and turbulence fields of the Strait of Dardanelles in order to better understand the specific hydraulic regime of this strait.

2 Model Description

The model is based on the 3D Reynolds-averaged Navies-Stokes equations and the Boussinesq approximation. The concept of eddy viscosity and diffusivity is used with a two-equation $k-l$ model of turbulence (Mellor and Yamada, 1982) to define turbulent stresses

and scalar fluxes. A generalized vertical coordinate for the vertical direction (Pietrzak et al. 2002) and orthogonal curvilinear coordinates in the horizontal directions are used in the model. Scalars, free surface elevation, hydrostatic and non-hydrostatic components of pressure and velocity are calculated at sequential stages. Unlike most of non-hydrostatic models, 2D depth-integrated momentum and continuity equations were integrated explicitly with the mode splitting technique at first stage, whereas the 3D equations were solved implicitly at subsequent stages. This approach is particularly advantageous for the shallow stratified flows and it is fully compatible with the POM model (Blumberg and Mellor, 1987). The finite-difference solutions of governing equations were derived using a four-stage procedure:

1 stage: Scalar fields.
The scalar fields (temperature and salinity), turbulent energy and length scale are computed by using a semi-implicit numerical scheme in the vertical direction. The obtained three-diagonal system is solved by a direct method.

2 stage: Free surface elevation.
The calculation of free surface elevation is performed explicitly from depth-integrated shallow water equations like in the POM model. The initial 2D velocity fields on each external stage are determined by direct integration of the general non-hydrostatic 3D velocity fields of the previous internal step.

3 stage: Hydrostatic components of the velocity and pressure fields.
The 3D hydrodynamic equations without the non-hydrostatic pressure are solved semi-implicitly (Casulli and Stelling, 1998) with an internal time step to determine provisional values of the velocity field. The advection and horizontal viscosity are discretized explicitly. The obtained three-diagonal system is solved by a direct method.

4 stage: Non-hydrostatic components of the velocity and pressure fields.
The non-hydrostatic components of velocity are computed by correcting the provisional velocity field with the gradient of non-hydrostatic pressure to satisfy the continuity equation for the sum of hydrostatic and non-hydrostatic velocities. The obtained discretized Poisson equation for the non-hydrostatic pressure is reduced to a non-symmetric 15-diagonal linear system. The preconditioned biconjugate gradient method is used to solve this system. Once the non-hydrostatic pressure is determined the corresponding components of velocity fields are calculated.

3 Results

3.1 Mixing in lock-exchange flows

The lock-exchange flows arise when removing the vertical barrier that separates two sub-basins that are part of a rectangular basin initially filled with a water of different density. This problem was studied mainly in the frame of an internal hydraulics approach, yet experiments show that these flows are highly unstable and result in the mixing between the two fluids (Hacker et al., 1996). With the use of a non-hydrostatic model the lock-exchange flow was simulated in a rectangular channel with depth of H=10 cm, length of L=80 cm and width of A=15 cm. The channel was portioned into two compartments with a vertical barrier placed at a distance $x_0=L/2$ from the one end. They were filled with a water of different density. The reduced gravity is $g' = g\Delta\rho / \rho_0$=1 cm/c^2, where g is acceleration of gravity, $\Delta\rho$ is density difference between the two sub-basins, ρ_0 is a reference density. The simulations were performed on a grid with a spatial resolution of 400x10x100. The calculations were carried

out with an internal time step Δt_I=0.06 s and an external time step Δt_E=0.002 s. This computational configuration of channel flow was similar to the DNS simulation of Hartel et al. (2000) who used a spectral numerical model. In contrast to that work we simulated an internal gravity flow with a free surface. Fig. 1 shows the formation of Kelvin-Helmholtz instability that results in the formation of finite-amplitude billows, which appear similar to the experiment of Hacker et al. (1996) and the DNS simulations Hartel et al. (2000) (Fig.2). This example demonstrates the ability of the present model to reproduce quite well the shear instability developed in stratified flows that are not in hydrostatic equilibrium.

3.2 Exchange flows through long straits with a sill

Here, the exchange flow throughout a shallow and narrow strait connecting two deep and wide basins filled with water of different density is considered. Such flow was reproduced by the laboratory experiment 701 of Maderich (2000), which was then numerically simulated. The laboratory strait is 60.5 cm long with two deeper and broad basins and with a rectangular cross section of maximal depth H=8 cm and constant width A=0.9 cm. The strait has a sill at its center with a ratio h/H=0.5. A buoyancy flux between the two basins was maintained by heating the left basin and cooling the right. It was simulated by including source and sink terms $SS_T=(T-T^*)/t^*$ in the heat transport equation. In the left and right basins T^* are $T_0+0.5\Delta T$ and $T_0-0.5\Delta T$, respectively. Here T_0 is the average temperature and ΔT is temperature difference, t^* is the relaxation time. The computations were carried out on a grid with resolution 200x11x60 in the curvilinear coordinates (Fig. 3). In numerical configuration the strait exits are smooth (Fig. 3), whereas in laboratory experiment, the strait exits had abrupt rectangular junction to sub-basins. The internal step was 0.02 s and the ratio of internal to external time step was 25. The composite Froude number G is calculated as:

$$G^2 = F_1^2 + F_2^2 \equiv \frac{u_1^2}{g' h_1} + \frac{u_2^2}{g' h_2},$$

where u_1, h_1 and u_2, h_2 are the velocity and thickness of the upper and bottom layer, respectively. The experiment and computations show that composite Froude number was closure to critical number over the sill, whereas the values of G were lower at the ends of strait (Fig. 4).

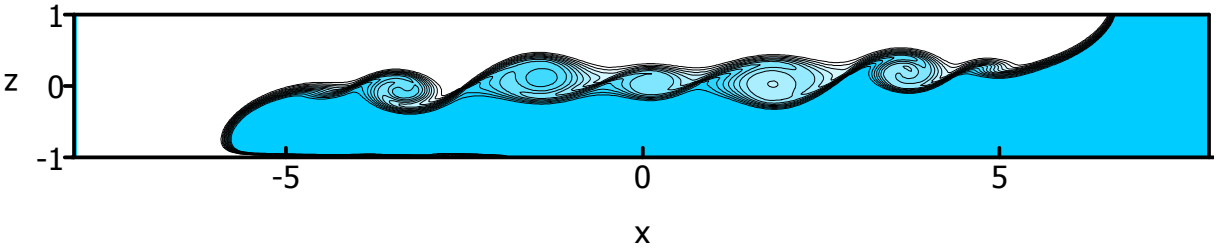

Figure 1: Density contour plot from the non-hydrostatic simulation with no-slip condition at the bottom and a free surface.

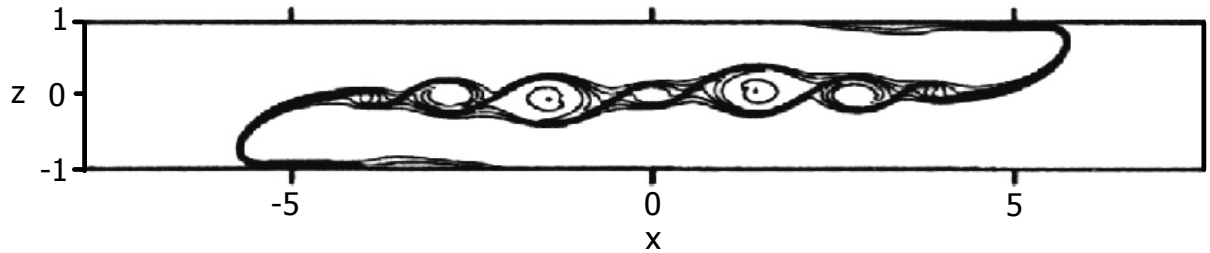

Figure 2: Density contour plot from the DNS simulation with no-slip symmetrical condition adapted from Hartel et al. (2000).

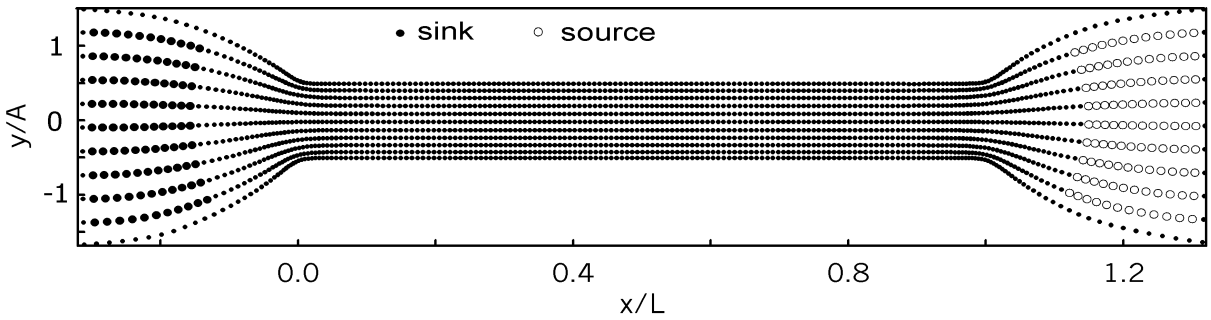

Fig3. Curvilinear coordinate grid: horizontal view of channel.

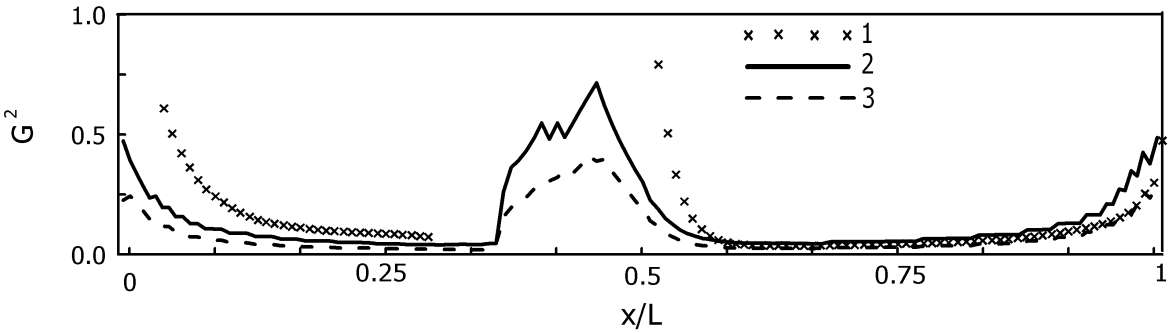

Figure 4: Composite Froude number along the strait calculated from the experiment 701 (1) vs. the computed one in the middle longitudinal section of the strait (2) and computed one using average flow parameters across the strait (3)

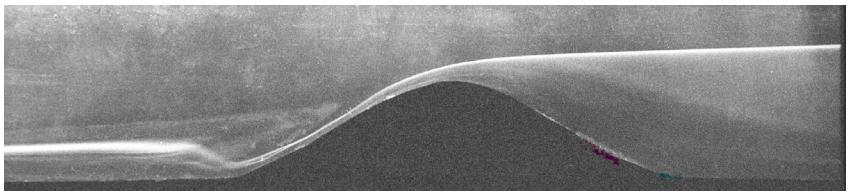

Figure 5: Photo of experiment 701.

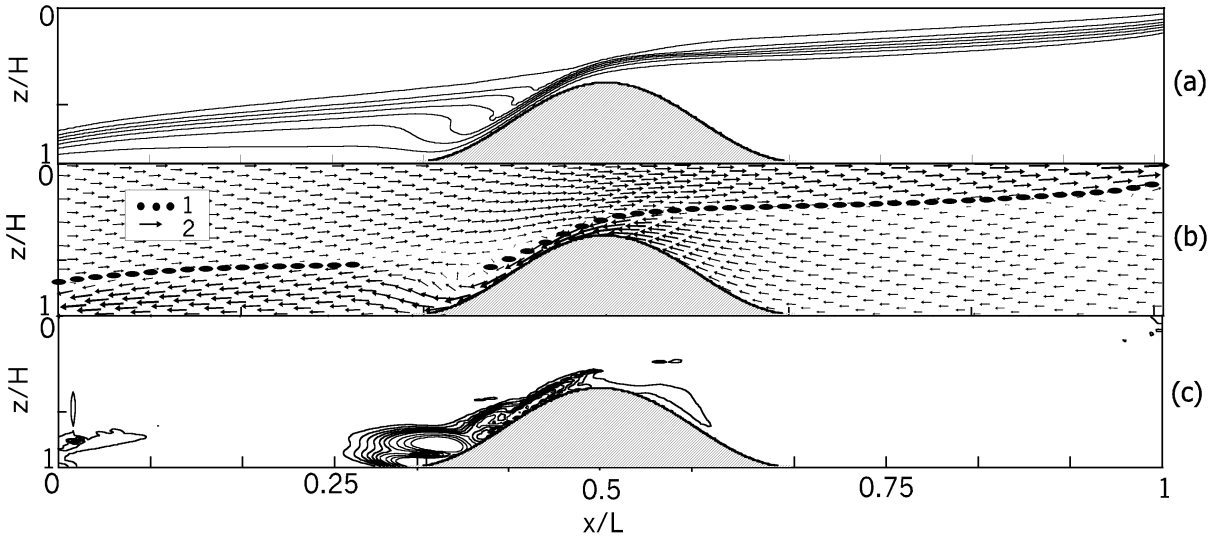

Figure 6: Computed density and velocity fields. (a) Contour plot of computed density from experiment 701. (b) Interface position in experiment 701 (1) and non-hydrostatic velocity field (2). (c) Absolute value of difference between hydrostatic and non-hydrostatic velocity fields.

The flow is laminar, however, measurements and computations showed broadening of the thermocline (Fig. 5, Fig. 6a). The detailed pattern of the velocity field shown in Fig. 6b indicates the presence of a complicated flow structure at the sill zone. The flow slows down at the left side of the sill and then creating a countercurrent. The dense water lifts along the left side of the sill and turns finally to the left, forming a broad interface layer. The broad thermocline is evidence of entrainment between the fluid layers. The entrainment and friction cause reduction the maximum values of G^2, computed by 3D non-hydrostatic model and displacing the locations of these values farther than expected from predictions of inviscid two-layer hydraulic theory. The comparison of non-hydrostatic and hydrostatic calculations was carried out with the same spatial resolution. Fig.6c indicates essential difference between non-hydrostatic and hydrostatic velocity fields. It is about 22% at the slope and the foot of the sill.

3.3 Exchange flows and mixing in the Strait of Dardanelles

The Strait of Dardanelles connects the Marmara and Aegean seas. It has an approximate length of 70 km, an average width of 4 km and an average depth of 55 m (Ünlüata et al. 1986). Its narrowest section with a width of 1.2 km occurs in the Nara Passage about 25 km east of the Aegean Sea. The flow is mainly driven by the salinity and elevation difference between the two seas. These differences are caused by the brackish water inflow from the Black Sea. The question regarding the flow regime of the Dardanelles is still open. Numerical simulations with the use of a two-layer model (Oğuz and Sur, 1989) and a vertically 2D non-hydrostatic model (Staschuk and Hutter, 2001) showed the presence of a submaximal exchange in the Strait controlled by the contraction at the Nara Passage. The bottom layer flow is subcritical throughout the Strait whereas the upper layer flow is supercritical in the Nara Passage (Staschuk and Hutter, 2001) and at the abrupt expansion of the width at its Aegean exit (Oğuz and Sur, 1989).

We simulated the exchange flows in a frame of a 3D model with *k-l* turbulence closure. The horizontal viscosity and diffusivity were set zero. The density difference was maintained by including a relaxation profile of salinity $SS_s = (S - S_s^*)/t_*$ in the salinity transport equation for the adjacent parts of the Aegean and Marmara seas. The summer conditions were simulated with zero net transport throughout the strait and no wind. The curvilinear horizontal grid was 160x15 with 50 sigma-levels in the vertical direction. The internal time step was 13.6 s and the ratio of internal to external time step was 20. The surface and near-bottom currents are given in Fig. 7. This figure shows a complicated field of currents caused by both the coast irregularities and bottom topography. A number of topographical gyres is also seen in the figure. The contour plots of density and turbulent energy are given in Fig. 8. The calculations show intensive mixing in the area of the narrowest section of the strait at the Nara Passage and southern of it. In previous studies (Ünlüata et al. 1986), the Nara Passage was identified as a hydraulic control place. The density interface rises to the Aegean exit indicating broadening of the pycnocline, which is caused by mixing between the layers. This figure conforms with distribution of turbulent energy which has a value of around 0.02 m^2s^{-1} at the contraction. The composite Froude number distribution is shown in Fig. 9. The Froude number now is lower than found in previous studies, even in the Nara Passage $G^2 < 1$. This finding, however, agrees with the estimate of G^2 in the Bosphorus strait by Gregg et al. (1999) on the basis of direct measurements. The numerical simulations of turbulent exchange flow through the contraction by Hogg et al. (2001), also demonstrated that mixing efficiently diminish G^2. It seems, that a zone of strong turbulence in the Nara Passage can limit the exchange, even though flow remains subcritical.

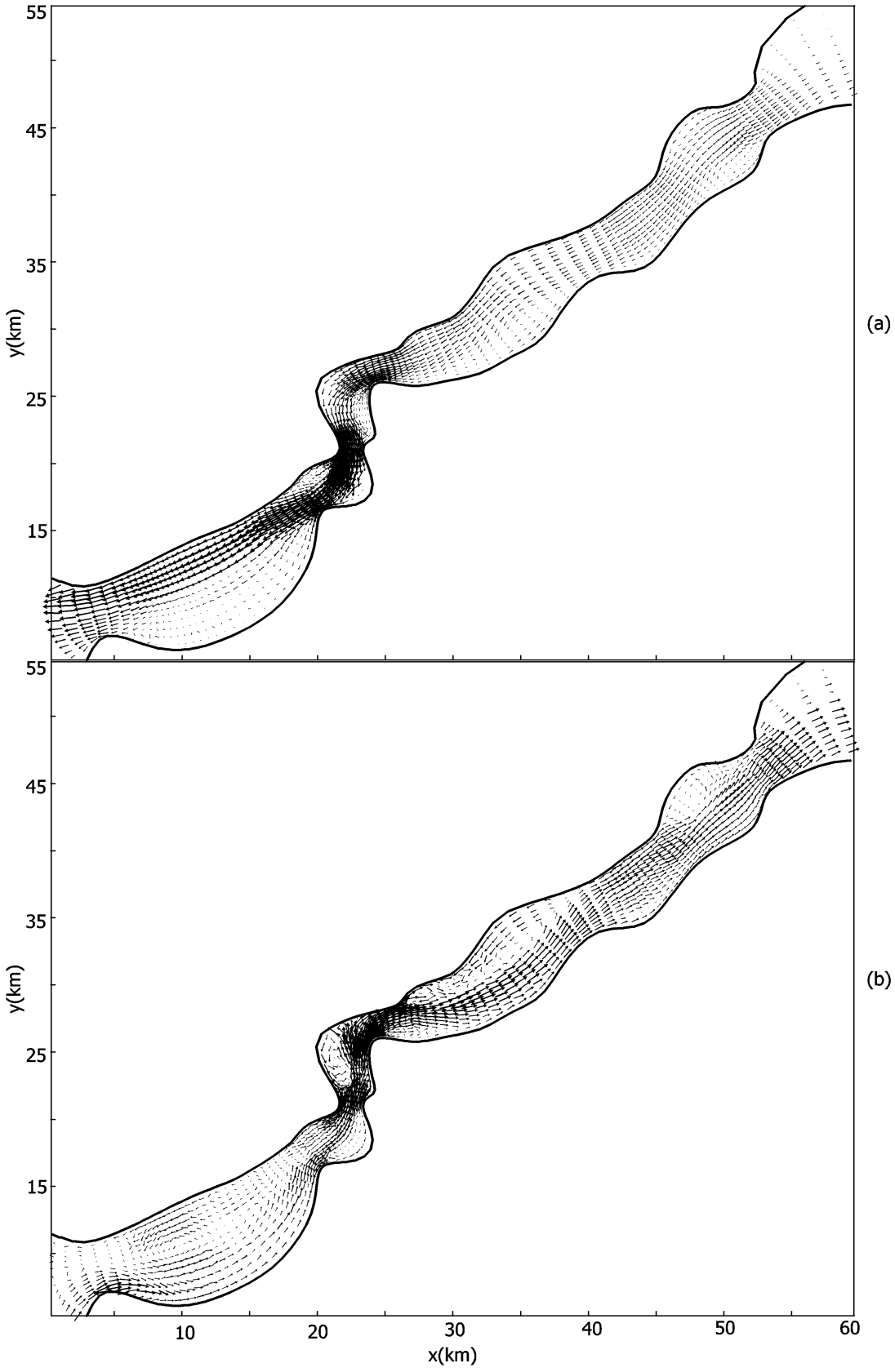

Figure 7: Velocity field (a) at the surface, (b) near the bottom.

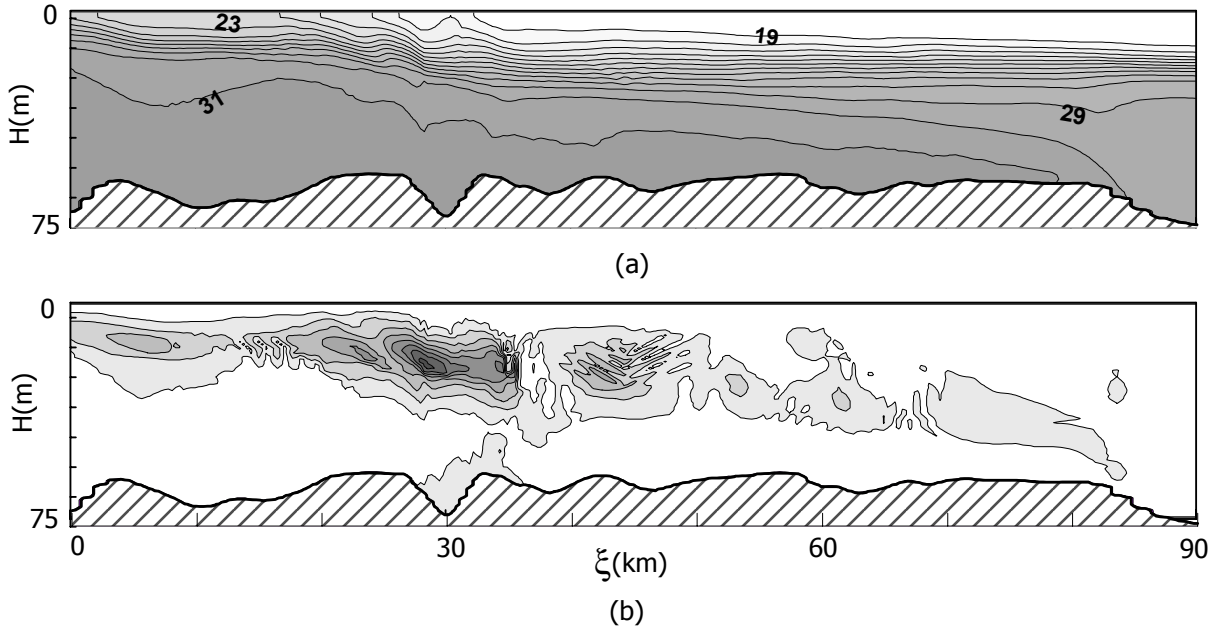

Figure 8: Contour plots of density σ_t (a) and turbulent energy (b) in the middle curvilinear longitudinal section through the Dardanelles.

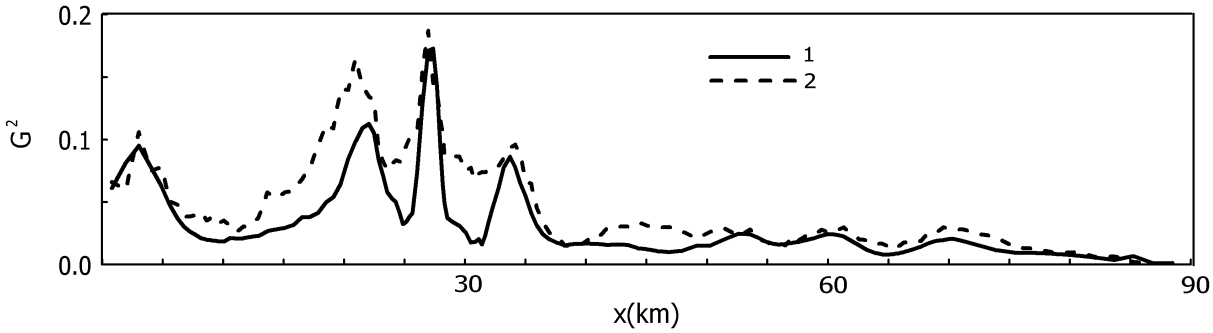

Figure 9: Composite Froude number calculated from average parameters across the Dardanelles (1), in the middle curvilinear longitudinal section (2).

Conclusions

The new three-dimensional, non-hydrostatic, numerical model of free-surface, unsteady, stratified flows developed by Kanarska and Maderich (2002a,b) was applied to investigate mixing in the lock-exchange flows and exchange dynamics in sea straits. The model was tested against laboratory experiment replicating the exchange flow through a long and narrow strait and the DNS simulations of the lock-exchange flow. The agreement was generally fair. The simulations demonstrate the ability of the present model to reproduce quite well the mechanism of shear instability in stratified flows that are far from being in hydrostatic equilibrium. The circulation in the Strait of Dardanelles was investigated in order clarify the role of mixing in exchange during the summer period with zero net transport. The model reproduces the complicated three-dimensional structure of currents in the strait. Calculated 3D fields of currents, density and turbulence intensity all show the effects of intensive mixing at the zone of the Nara Passage. It was found that, contrary to previous studies, the composite Froude numbers were subcritical along the strait. It is concluded that mixing can play a crucial role in limiting the exchange throughout the Dardanelles. More detailed field studies and simulations are necessary in the future to understand the processes in the Nara Passage area.

Acknowledgements
This study was partially supported by US Civil Research and Development Foundation (Contract UG2-2425-SE-02), bilateral Greek-Ukrainian collaborative project "The Black and Aegean seas interaction and exchange: an integration of in-situ measurements, satellite data and numerical modeling" and INTAS Fellowship for Young Scientists № YSF 2002-127 (Yuliya Kanarska). The article benefited from comments and suggestions of an anonymous referee.

References

1. Armi L., Farmer D.M. (1986) Maximal two-layer exchange through a contraction with barotropic net flow. *J. Fluid Mech.* 164, 27-52.
2. Blumberg A.F., Mellor G.L. (1987) A description of a three-dimensional coastal ocean circulation model, in N.S. Heaps (ed.), *Three-Dimensional Coastal Ocean Circulation Model*s, *Coastal and Estuarine Science*s, vol. 4, AGU, Washington, DC, pp. 1–16.
3. Casulli V., Stelling G. S. (1998) Numerical simulation of 3D quasi-hydrostatic, free-surface flows. *J. Hydr. Eng.* 124, 678-686.
4. Farmer D.M., Armi L. (1986) Maximal two-layer exchange over a sill and through the combination of a sill and contraction with barotropic flow. *J. Fluid Mech.*164, 53-76.
5. Gregg M.C., Öszoy E., Latif M. (1999) Quasi-steady exchange flow in the Bosphorus. *Geoph. Res. Let*. 26, 83-86.
6. Hacker J., Linden P. F., Dalziel SB. (1996) Mixing in lock-exchange gravity currents. *Dyn. Atmos. Oceans,* 24*,* 183-195.
7. Hartel C., Meiburg E., Necker F. (2000) Analysis and direct numerical simulation of the flow at a gravity-current head. Pt1. Flow topology and front speed for slip and no-slip boundaries. *J. Fluid Mech*. 418, 189-212.
8. Hogg A., Ivey G., Winters K. (2001) Hydraulics and mixing in controlled exchange flows. *J. Geoph. Res.* 106*,* 959-972.
9. Kanarska Y., Maderich V. (2002a) Non-hydrostatic model for stratified flows with free-surface. *Appl. Hydromech.* 4(76), No.3, 12-21.
10. Kanarska Y., Maderich V. (2002b) A non-hydrostatic numerical model for calculating of free-surface stratified flows. *Ocean Dynamics* (Submitted).
11. Maderich V. S. (2000) Two-layer exchange flows through long straits with sill. *Oceanic Fronts and Related Phenomena. Konstantin Fedorov Int. Memorial Symp., IOC Workshop Rep. Series***,** N 159*,* UNESCO'2000, 326-331.
12. Mellor G. L., Yamada T. (1982) Development of turbulence closure model for geophysical fluid problems. *Rev. Geophys. Space. Phys*. 20 No. 4, 851-875
13. Oğuz, T., Sur H. (1989) A two-layer model of water exchange through the Dardanelles Strait. *Oceanologica Acta* 12, 23-31.
14. Pietrzak J, Jakobsen J. B., Burchard H., Vested H. J., Petersen O. (2002) A three-dimensional hydrostatic model for coastal and ocean modelling using a generalised topography following co-ordinate system. Ocean Modelling 4, 173-205.
15. Staschuk N., Hutter K. (2001) Modelling of water exchange through the Strait of Dardanelles*. Cont. Shelf. Res.* 21, 1361-1382.
16. Ünlüata Ü., Oğuz T., Latif M. A., Öszoy E. (1990) On the physical oceanography of the Turkish Straits. In *The Physical Oceanography of Sea Straits* (Pratt, L.J., ed.) NATO/ASI Series, Kluwer Academic, Netherlands, 25-60.
17. Zhu D.Z., Lawrence G. A. (1998) Hydraulics of exchange flows. *J. Hydr. Eng.* 126*,* 921-928.